Available online at www.sciencedirect.com
SCIENCE DIRECT®
Applied Clay Science 23 (2003) 299–308
Applied CLAY Science
www.elsevier.com/locate/clay

Quantitative analysis of anatase in Georgia kaolins using Raman spectroscopy

Paul A. Schroeder[a,*], Nathan D. Melear[a], Robert J. Pruett[b]

[a] *Department of Geology, University of Georgia, 210 Field St. Room 132, Athens, GA 30602-2501, USA*
[b] *IMERYS Pigments and Additives Group, Sandersville, GA 31082, USA*

Received 11 July 2002; accepted 15 April 2003

Abstract

Raman spectroscopy of Georgia kaolins ubiquitously show a strong E_g frequency near 144 cm^{-1}. Analysis of the band intensity shows that under specific source, sample, and optical conditions, peak area measurements are predictable and reproducible. Using standard additions, successful quantitative techniques have been developed that allow analysis of 25% solids water slurries, which achieve anatase detection limits down to 0.3% with a standard error of $\pm$ 0.1%. Anatase was also studied with X-ray powder diffraction to examine the extent of crystal chemical variation. The *a* lattice dimensions of anatase from Georgia kaolins range from 0.3786 to 0.3796 nm. The mean coherent scattering length in the [100] direction range from 80 to 160 nm. Given the range of anatase particle sizes previously observed in Georgia kaolins (8000–150,000 nm), these parameters indicate an average defect density of 100 domains per crystal and structural formulae that range from $Fe_{0.03}Ti_{0.97}O_{1.97}(OH)_{0.03}$ to $Fe_{0.06}Ti_{0.93}O_{1.93}(OH)_{0.06}$.

Quantitative estimates of anatase abundance using Raman require careful attention to background fluorescence effects due to the presence of hematite, goethite, and organic matter. Background fluorescence intensity in the regions of 400 and 600 cm^{-1} correlate with known additions of hematite and goethite, respectively. The removal of organic matter from gray clays by H_2O_2 treatment significantly reduced background fluorescence. The small variations in anatase crystal chemistry do not appear to have any first-order effects on Raman intensity of the 144 cm^{-1} band.

The comparison of total TiO_2 using X-ray fluorescence techniques with anatase content reveals that, in many instances, there is a significant non-anatase TiO_2 component present in Georgia kaolins. The discrimination of Ti-phases has the potential to provide new insights into strategies for mineral separation techniques, kaolin reserve estimates, and understanding of the geologic history of the Georgia kaolin deposits.

Keywords: Raman; Anatase; Rutile; Ilmenite; X-ray diffraction

1. Introduction

Quantitative assessment of Ti-bearing phases in Georgia kaolins is an essential step in determining mineral processing strategies for kaolin ore and its subsequent use in the paper, paint, filler, and pharma-

* Corresponding author. Tel.: +1-706-542-2384; fax: +1-706-542-2425.
E-mail address: schroe@uga.edu (P.A. Schroeder).

0169-1317/03/$ - see front matter © 2003 Elsevier B.V. All rights reserved.
doi:10.1016/S0169-1317(03)00129-7

ceutical industry. The most common industry method used for assessing the Ti content is X-ray fluorescence spectroscopy (XRF). The XRF method provides both accurate and precise measures of the total amount of Ti in a sample. Unfortunately, the total Ti content (often reported as weight percent TiO_2) does not discriminate between the various Ti-bearing phases commonly found in kaolins. More precise knowledge of Ti-phase abundance and crystal chemistry may also make more efficient the mineral separation methods used in the kaolin industry (e.g., magnetic, floatation, and selective flocculation) as well as give insights to the geologic evolution of the Georgia kaolin deposits.

Murad (1997) and Murad and Köster (1999) first suggested Raman spectroscopy as a viable method for characterizing anatase in kaolins. They duly noted that the technique of X-ray diffraction (XRD) could only quantify anatase in kaolins down to a limit of about 0.5 wt.%. Schroeder and Shiflet (2000) verified their estimate by using XRD to discriminate anatase from non-anatase TiO_2 in an east Georgia kaolin. Schroeder and Shiflet (2000) also indicated that rutile and a heterogeneous nano-crystalline phase constitute quantitatively important forms of the non-anatase TiO_2 measured by XRF. Given the fact that the TiO_2 content of Georgia kaolins can vary from 0.1 to 7 wt.% and the need to more clearly delineate non-anatase forms of Ti, it is now recognized that more streamline (i.e., less labor-intensive) and discriminating techniques are needed for the characterization of Ti in Georgia kaolins. The purpose of this paper is to describe approaches and considerations for using Raman spectroscopy to quantifying anatase in Georgia kaolins.

2. Materials and methods

2.1. Samples

The samples used for this study include kaolins from the published studies by Schroeder and Pruett (1996), Schroeder et al. (1998), and a series of kaolins representative of both the east and central Georgia mining districts (see Table 1). Standard addition experiments (described below) included the use of synthetic anatase, synthetic goethite (Schwertmann and Cornell, 1991) and hematite from Graves Mountain, GA (Schroeder, 1999).

2.2. X-ray diffraction and chemical analysis

XRD analyses were conducted using a Scintag XDS-2000 diffractometer, solid-state detector, and Cu radiation source. Back-filled pressed sample mounts were made to minimize transparency and sample displacement effects, as discussed by Hurst et al. (1997). Quantitative analysis for anatase content was performed using the internal standard method (ZnO) and is thoroughly discussed in Schroeder and Shiflet (2000). The methodology for indexing and unit-cell refinements of the anatase is also described in Schroeder and Shiflet (2000). In brief, samples were digested to remove kaolinite with 5 N NaOH using the method of Kampf and Schwertmann (1982) as modified by Singh and Gilkes (1991). Halite was added as an internal standard to digestion residuum to determine the anatase lattice parameters and mean coherent scattering length according to the Scherrer equation (Klug and Alexander, 1974). Selected samples were also treated for the removal of Fe-oxide phases using citrate–dithionite–bicarbonate (CDB) solutions and removal of organics using H_2O_2 according to the method described in Schroeder and Ingall (1994).

Quantification of elements was accomplished by analyzing fused discs with a Philips PW1480 X-ray fluorescence spectrometer (XRF) equipped with a Sc/Mo dual anode source. Kaolin color and brightness was measured using a Technibrite Micro TB-1C instrument on dried and pulverized powder that is pressed with 2.07 bar pressure (30 psi) to form a flat surface for analysis.

2.3. Raman spectroscopy

The phenomenon of Raman scattering has been recognized for over seven decades (Raman and Krishnan, 1928); however, to date, there are few published works regarding its application to quantification of phases in kaolins. To understand how Raman spectroscopy may be applied to quantitative problems, it is vital to know how the intensity, directional properties, and state of polarization of Raman scattering are related to components in the scattering system (Long, 1977). Raman scattering is different

Table 1
Mineral suites and specimens used in Raman study

Locality	ID code	Fe_2O_3	TiO_2	Hinckley index[a]	Crude brightness	L	a	b
Hall cream	HC	0.55	1.45	0.38	77	92.1	− 0.22	6.27
Hall pink	HP	1.20	1.50	0.46	68	88.5	2.83	8.37
Hall gray	HG	1.41	1.42	0.33	62	83.9	0.41	7.55
Central GA	TH	0.66	1.99	0.73	62	83.4	0.61	7.11
Central GA	HO	0.37	1.99	0.95	78	92.7	− 0.17	6.26
Central GA	DC	1.17	1.35	0.53	75	88.8	− 0.05	3.61
Central GA	T1	1.43	1.62	0.52	60	82.4	3.13	7.21
Central GA	T2	1.23	1.41	0.95	60	82.9	1.33	7.75
Central GA	TT	0.51	1.62	1.14	71	88.8	1.48	6.66
East GA	CC	0.90	2.54	0.29	74	92.2	− 0.38	8.88
East GA	PT	0.78	3.27	0.25	78	92.5	− 0.18	6.49
East GA	PB	1.08	1.48	0.43	81	94.1	− 0.43	5.92
East GA	PO	1.01	2.84	0.40	71	89.3	2.53	6.93
Central GA	KG	0.38	1.79	1.13	85	95.3	− 0.29	4.93
East GA	TG	1.11	2.38	0.51	79	92.8	1.34	5.83
Brazil	RC	0.80	2.23	1.42	77	91.1	1.85	5.02
Brazil	TC	1.81	1.17	0.39	n.d.	n.d.	n.d.	n.d.
Australia	SC	1.30	1.54	0.33	n.d.	n.d.	n.d.	n.d.
Indiana US	WG	0.11	0.01	1.72	n.d.	n.d.	n.d.	n.d.
Central GA	KC	0.47	2.45	0.84	n.d.	n.d.	n.d.	n.d.
Pugu Hills	PH	1.31	0.98	0.39	n.d.	n.d.	n.d.	n.d.

Top group includes samples representative of central Georgia mining district. The middle group is representative of east Georgia mining district. The bottom group includes samples from Schroeder and Pruett (1996) and Schroeder et al. (1998). Also included are relevant chemical, crystal, and color data. Color data defined by Lab system where L = lightness/darkness value (100 → 0), a = hue (− a → green, + a → red), and b = chroma (− b → blue, + b → yellow).

n.d. = no data.

[a] Crystallinity index measure according Hinckley (1963).

from infrared absorption phenomenon (i.e., Beer's law) in that it is orders of magnitude less efficient of a process. Consequently, use of the signal for quantification can be difficult. However, in well-defined systems, using internal standards for calibration and with careful monitoring of experimental conditions (laser power, sample presentation, and detector angle) spectral band intensities can be quantitatively related to components with high scattering efficiencies (Vickers and Mann, 1991).

Previous works, Murad and Köster (1999) and Murad (1997), have demonstrated that commercial Raman spectrometers offer a viable means for characterization of anatase in kaolins. The key parameters needed to be carefully considered in a quantitative Raman experimental setup include: (1) the adjustment of laser power levels and monitoring of laser output stability; (2) the duration of data collection as it affects (a) the number of co-added scans that can be obtained to improve signal to noise and (b) the amount of thermally induced fluorescence or thermoluminescence that can add to signal background; and (3) sample mounting methods, which can be accomplished in either powder or slurry form (Vickers and Mann, 1991).

Quantitative Raman spectroscopy for this study was conducted using a Nicolet FT-Raman 950 spectrometer. This spectrometer employs a near-infrared 5 W multi-mode Nd:YAG diode laser operating at 1064 nm with continuous, variable attenuation, capable of delivering power to the sample in the range of 0.02–1.2 W. Detection is by a Michaelson interferometer and an InGaAs detector. Preliminary experiments were conducted to examine the relationship between the absolute intensity of the Raman active anatase E_g mode (v_6 = 144 cm^{-1}, Ohsaka et al., 1978) in a kaolin sample and the spectrometer laser power. Over the range of 0.05–0.25 W, the scattering intensity response was measured to be linear with a correlation of r^2 = 0.99. Subsequent quantitative experiments

were run with the laser power at a constant set value in the power range above (see individual figure captions for experimental parameters).

Preliminary experiments were conducted to examine the effects of excitation time of the 1064 nm laser, as it well known that FT-Raman is compromised by the v^4 power dependence (e.g., using 523 nm excitation requires 16 times less power than 1064 nm excitation; Vickers and Mann, 1991). Repeated bombardment by the laser source can result in local heating, thus adding a thermoluminescence component to the spectrum. Spectral data were co-added over a range from 10 to 10,000 scans to examine the effects of heating and instrument drift. Our preliminary results indicated that water-slurried experiments and dry-powdered experiments showed minimal added thermoluminescence background response with additional number of scans (i.e., beyond 2048). Scans in the range of 64–2048 produced comparable signal-to-noise. It is important to point out that a consistent background correction method be employed when quantifying the anatase 144 cm^{-1} peak. Rayleigh scattering can be four to five orders of magnitude more intense and therefore impart a tail effect on the low frequency region. The spectra in this study were well defined enough (i.e., 144 cm^{-1} peak width at half height = 10 cm^{-1}) to allow the selection of 100 cm^{-1} as the low wave number cutoff point for baseline correction.

In an effort to evaluate the use of slurries, dry kaolin was combined with water and Na-hexametaphosphate, and then pH adjusted using small additions of 1 N NaOH. A series of dispersed 3, 10, 15, 20, 25, 30, 40, and 50 wt.% solids were made. The constant pH level was selected for three reasons. Firstly, pH control allows for consistent dispersion of the particles in solution, which in turn should enhance the Raman scattering effect. Secondly, Johnston et al. (1985) noted an increase in the Raman intensities of the 3600–3725 cm^{-1} band region (OH stretching) with increasing solution pH. The presence of additional OH^- groups near the surface of kaolinite crystals may influence the polarizability of the hydroxyl groups on surface of kaolinites. We, however, did not critically evaluate the OH region in our study. Finally, the dispersion treatment is similar to that used for the industrial processing of kaolins and, therefore, allows for assessment of the potential for direct measurement on kaolin slip.

3. Results and discussion

3.1. Evaluation of kaolin slurries

Fig. 1 shows the Raman intensity of the anatase at 144 cm^{-1} band versus the percent solids in sample KG, which contains 2.45 wt.% TiO_2. For slurries with ≤ 3% solids, high levels of background relative to signal made conditions unreliable for quantification. Between 3% and 30% solids, the spectral response is quasi-linear. Above 35% solids, the signal is constant. We chose an optimized fit of all the data using a sigmoid function. The reasonably good correlation ($r^2 = 0.99$) demonstrates that the Raman method has the potential to be calibrated to solids content (if anatase is known) or calibrated to anatase content (if percent solids is known). Potential users of this method must realize that the shape curve in Fig. 1 may change if different Raman instrumental parameters are used.

3.2. Quantification of anatase using Raman spectroscopy

Fig. 2 shows an example of spectral response due to standard additions or "spiking" along with a plot of

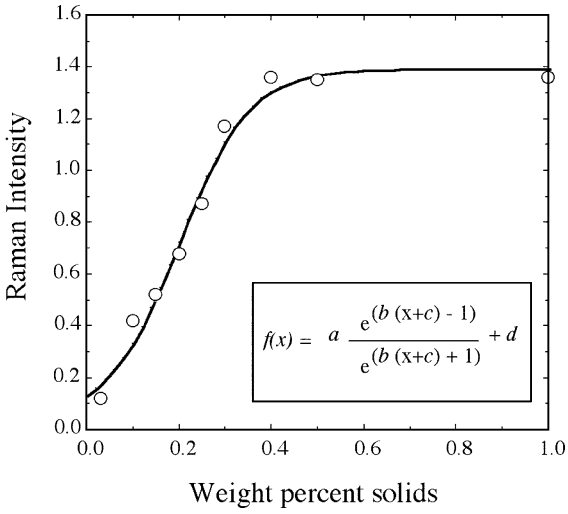

Fig. 1. Raman intensity at 144 cm^{-1} plotted as a function of percent solids in a kaolin slurry. Concentration of anatase in dry kaolin is approximately 1 wt.%. Data collected with 256 scans and laser power = 0.05 W). The line represents a least-squares optimization using a sigmoid function (Raner, 1998). Coefficients corresponding to the best fit are $a = 0.67$, $b = 13.2$, $c = -0.20$, and $d = -0.72$.

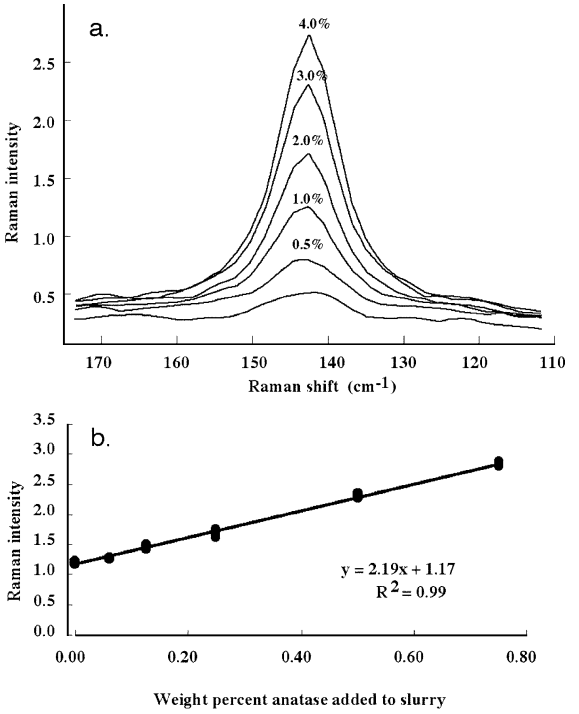

Fig. 2. (a) Raman spectra showing 144 cm^{-1} peak of slurries sample with standard additions ranging from 0 to 4 wt.% anatase. Data collected with 256 scans, laser power = 0.125 W, and background correction. (b) Raman intensity at 144 cm^{-1} plotted as a function of weight percent synthetic anatase added to anatase-bearing kaolin slurry. Using the internal standard method of Skoog et al. (1998), the sample contains 2.1 ± 0.1 wt.% anatase.

intensity versus percent anatase added to the slurry. A synthetic anatase was chosen because independent X-ray diffraction analysis indicates the X-ray scattering domain size distributions are similar to those in the naturally occurring anatase (note: XRD discussion below will further address the crystallinity of the natural anatase). Standard additions were made to 25% slurries of sample TG and 20% slurries of sample KG, using the method of Skoog et al. (1998). A minimum of four replicate data points was used for each sample. High correlations ($r^2 = 0.98$) are observed with a linear regression fit. Error was calculated using the following equation,

$$\text{absolute\_error} = \text{wt.\%}\sqrt{\left(\frac{e_b}{b}\right)^2+\left(\frac{e_m}{m}\right)^2} \quad (1)$$

where wt.% = concentration of analyte, b = intercept, m = slope, e_b = standard error of y, and e_m = standard error of x coefficients. The concentration of anatase in the water-free state of TG is 2.1 ± 0.1% and for KG is 1.5 ± 0.3%. In both cases, the E_g Raman active mode at 144 cm^{-1} revealed a linear intensity response and similar error values.

The effect of the common kaolin ore components, hematite and goethite, on the intensity of the anatase band was evaluated by making standard additions of hematite and goethite to sample KG. Initial studies of hematite standard additions to kaolinite suggested that there was the potential to discriminate minor amounts of hematite by the presence of two A_g and five E_g modes at 226, 293, 245, 299, 412, and 612 cm^{-1} (Beattie and Gilson, 1970; Bersani et al., 1999). Upon numerous subsequent Raman studies, our results indicate that discreet bands for the minor phase hematite are most often obscured by background components. However, background levels respond in a systematic manner that can be generally described as increasing intensity with increasing content of Fe-bearing or natural organic compounds. Fig. 3a–c shows background intensities increase with the addition of Fe-bearing phases or decrease with the removal of Fe-bearing phases. This change in background is ascribed to a broadband thermo-fluorescence effect that is induced by continued energy input from the laser source into the sample.

Particle size effects appear to be important in the case of hematite. Hematite bands can be resolved in dilute (~ 1 wt.% dry powder) concentrations, only when a well-crystalline and large particle size hematite is added, such as the Graves Mountain hematite used in this study. However, as the particle size becomes smaller (like the hematite found in most kaolin deposits), the ability to resolve bands becomes diminished. When using the Raman experimental conditions for the anatase quantification, it was not possible to detect hematite bands. Hematite bands were only resolved in the reddest sample, TT, after using numerous co-additions of the data.

Spectral responses observed with standard addition experiments using goethite did not reveal discrete bands attributable to goethite (de Faria et al., 1997). Given that goethite particles are extremely small, the opportunity to detect specific bands in kaolinite-rich samples appears nonexistent. Like hematite, we are encouraged about the systematic response of the

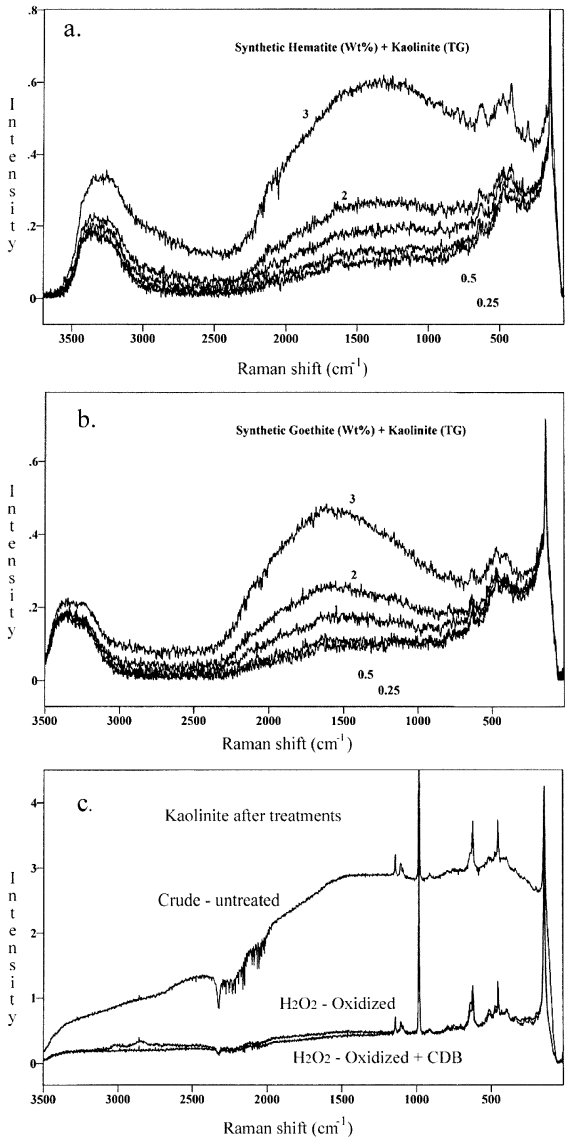

Fig. 3. Raman spectra of sample TG slurries (25% solids) with standard additions of iron phases. Note added thermoluminescence contribution to background with increasing amounts of iron. (a) Standard additions of synthetic hematite ground from Graves Mountain, GA. (b) Standard additions of synthetic goethite. (c) Raman spectral response of a TG crude powder before and after sequential treatment for removal of organic carbon (30% H_2O_2) and extraction of iron using the CDB method. K_2SO_4 (982 cm^{-1}) added as an internal standard (1:2) to check for instrument response intensity. Laser power = 0.15 W, 2048 scans.

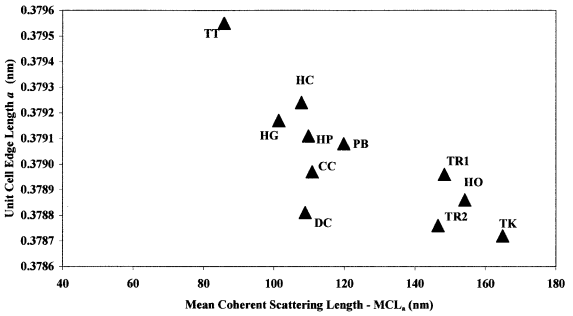

Fig. 4. Mean coherent scattering length of the anatase in Georgia kaolins. The MCL_a parameter is specific to the [100] direction in the lattice, which is the same direction as the *a* unit cell edge. Dimensions of the *a* unit cell length were determined by indexing of the anatase (101), (103), (004), (112), (200), (105), and (211) reflections. The mole fractions of Fe = Fe/(Fe + Ti) (mol mol^{-1}) in anatase are estimated using the best-fit solution to soil data of Schwertmann et al. (1995).

background level to the changing presence of goethite (Fig. 3b).

Also documented is the large effect of organic matter removal has on decreasing the background level. Fig. 3c shows clearly the reduction in background as a consequence of treatment by H_2O_2. The removal of Fe-rich phases by CDB treatment also lowers the background scatter, however, to a much lesser extent. The absolute intensity of the uncorrected background for hematite and goethite standard additions at 400 and 600 cm^{-1}, respectively, linearly increase with increasing additions. Correlations (r^2) for the fit of intensity versus weight percent added (plot not shown) for hematite and goethite are 0.90 and 0.96, respectively.

3.3. X-ray diffraction analysis of anatase

The ability to quantify anatase using Raman spectroscopy is potentially limited if there are significant variations in the anatase particle size and composition. The crystalline habit of anatase in Georgia kaolins has been described as a pseudo-cubic form with edges that range from 80 to 120 μm (Schroeder and Shiflet, 2000; Hurst et al., 1997; Weaver, 1976). Using the Scherrer equation (Klug and Alexander, 1974), Fig. 4 shows that the mean coherent scattering length in the *a* direction ranges from 80 to 170 nm.

The dimensions of the anatase unit cell are known to vary as a function of isomorphous Fe substitution for Ti. Schwertmann et al. (1995) have also shown that mole fraction of Fe in anatase is positively correlated with the *a* lattice parameter. Using the concentrate samples (i.e., kaolinite removed), it was possible to index the anatase diffraction data, such as that shown in Fig. 5. The *a* lattice parameters determined from the study samples were used with Schwertmann's et al. (1995) relationship to estimate the amount of Fe substitution (Fig. 4) These estimates of mole fraction of Fe in anatase from Georgia kaolins range from 0.03 to 0.06. This supports the notion that as Fe substitution increases, the crystal defect density of the anatase increases.

The variations in anatase Fe content and crystallinity can potentially affect the Raman spectral response (Vickers and Mann, 1991). The XRD peak shapes of the natural anatase appear very similar to those of the synthetic anatase used for the spiking. The average anatase coherent scattering length is about 100 nm. As noted above, the average crystal size is about 0.1 μm (10,000 nm), thus indicating a relatively low defect density (i.e., ~ 100 domains per crystal). Whether or not there is a relationship between particle size, crystal defect density, and Raman response remains unknown. Farmer (1998) notes that lower symmetry crystals without a center of symmetry that are thick relative to the excitation wavelength ($\lambda = 1064$ nm in this study) potentially have Raman active optical modes. Anatase has a center of symmetry (Ohsaka et al., 1978) and the particles are large in relation to λ. The extent of Fe substitution in Georgia anatase varies over a small range. Their defect density is smaller than λ. Therefore, is it assumed that intensity variations, due to factors such as induced optic modes, do not have a first-order impact on intensity measurements and quantification. Farmer (1998) also notes the importance of scattering geometry. In our study, the source and geometric conditions are kept constant so it is assumed that these factors are constant.

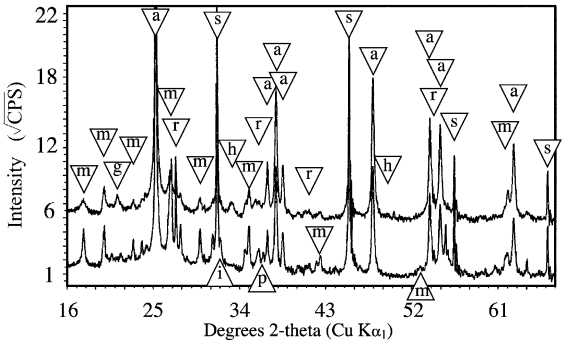

Fig. 5. X-ray powder diffractogram (Cu-Kα_2 stripped) of the HG and HP clay residual concentrate after NaOH digestion. Strong intensity reflections have been identified and labeled with the following symbols: (a) anatase, (g) goethite, (h) hematite, (i) ilmenite, (m) 2 M_1 illite, (p) pseudorutile, and (s) halite as an internal standard. Unlabeled peaks are subsidiary reflections of the phases above. Intensities are plotted as the square root of counts per second (CPS) to visually enhance smaller peaks.

3.4. Comparison of XRD and Raman quantification

Three samples from the C.F.I. Hall Mine series (cream kaolin—HC, pink kaolin—HP, and gray kaolin—HG) were selected for a quantitative comparison of anatase content. These were chosen because they all contained relatively similar TiO_2 contents (Table 1.) However, preliminary XRD analysis indicated that there were differences in anatase content amongst the three samples. The intent here is to highlight the concern that not all the TiO_2 in Georgia kaolins occurs as anatase.

Weight percentages of anatase derived by Raman spectroscopy were taken from the calibration of samples whose anatase mass was accurately known using the spiking method. Anatase content was plotted versus spectral band intensity and a least-squares line was fit to the data. For our particular setup (i.e., 25% solid slurries, 128 scans, and invariant laser power), this resulted in the equation $y = 1.691x$, where y is the weight percent anatase and x is the E_g (v_6), background-corrected band intensity at 144 cm^{-1}. Using this calibration, the percent anatase was determined directly for each of the C.F.I. Hall samples by measuring the band intensity at 144 cm^{-1}. Fig. 6 shows a plot of the weight percent anatase determined by XRD versus the same determined by Raman spectroscopy. The solid line represents a 1:1 plot. With exception of the HG sample, there is a very good agreement. Note that the total TiO_2 content for all samples is greater than maximum anatase value measured (1.4 wt.%). This indicates that either both techniques underestimate the anatase content or there are non-anatase

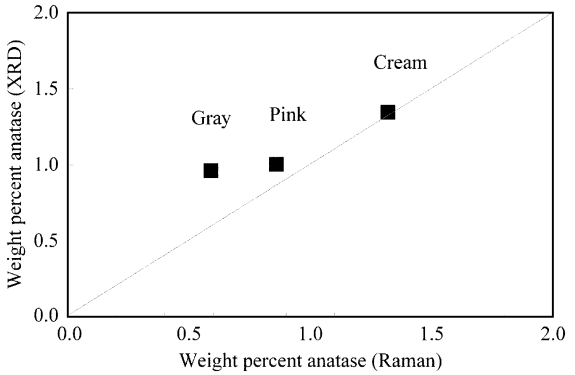

Fig. 6. Raman versus XRD results for quantification of anatase in the HG (gray kaolin), HP (pink kaolin), and HC (cream kaolin) series. The 1:1 slope line is presented for reference.

phases present in the samples. The non-anatase phases are likely rutile (Fig. 5) and nano-crystalline forms, possibly occurring as degraded ilmenite and pseudorutile, much like that seen in weathered strandline deposits (Grey and Reid, 1975). Raman bands of rutile (typically at 448 and 610 cm^{-1}) were not resolved in the spectra.

The gray kaolin sample falls off the 1:1 line. This indicates that either the XRD overestimates anatase content or Raman underestimates anatase content. The XRD method assumes constant instrument-, sample-, and specimen-sensitive parameters (Hurst et al., 1997), with only the abundance of the analyte changing slightly. The quantification of anatase by XRD is complicated by the anatase (101) peak at 3.52 Å that is overlapped by the much more intense kaolinite (002) peak at 3.57 Å (Murad and Köster, 1999). The model XRD peak profile shape function used to the quantify the areas of the two closely positioned peaks is a Lorentzian function (Howard and Preston, 1989), which likely does not exactly describe the observed peaks that are a convolution of many instrument and specimen functions (Klug and Alexander, 1974). As the area contribution of the anatase peak diminishes and kaolinite increases, the misfit between the observed and model functions becomes greater. This is the most reasonable explanation for the slight overestimate of anatase by XRD.

The potential to underestimate the anatase content in the gray kaolin by the Raman method could be brought about by an increased background caused by a slightly higher organic carbon content (as indicated by the gray color). The effect of added background due to the presence of iron oxides and hydroxide is not considered to be major factor, as the minor addition of hematite and goethite was seen not to significantly affect the intensity of main band at 144 cm^{-1} (see Fig. 3a and b). At this point in time, we consider that the Raman technique for quantifying anatase at low concentrations (~ 0.5%) is both a more precise and accurate technique than the XRD technique.

3.5. Excess TiO_2

The difference between total TiO_2 and anatase TiO_2, previously referred to as non-anatase TiO_{2v} is herein referred to as excess TiO_2. Calculation of the excess TiO_2 for all the study samples results in the plot shown in Fig. 7. It is clear to see that for kaolins from Georgia and kaolins from other parts of the world, all have TiO_2 contents that are equal to or greater than the amount of anatase. This result has important implications for (1) strategies for anatase removal during kaolin processing, (2) reserve assessments, and (3) the mineral reaction pathways followed during the geologic alteration history of kaolin deposits.

From a geologic perspective, Schroeder and Shiflet's (2000) quantitative measurement of Ti-bearing

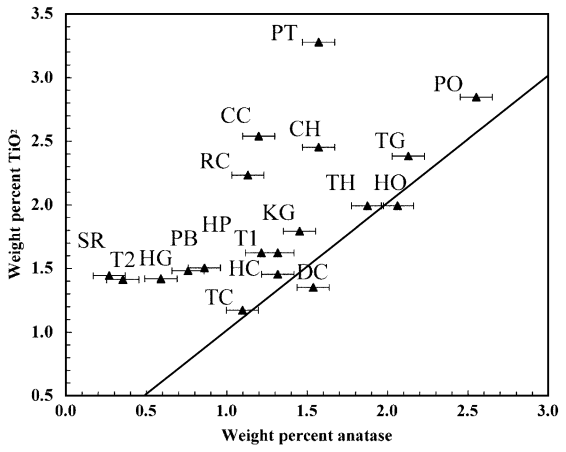

Fig. 7. Weight percent total TiO_2 (measured by XRF) versus weight percent anatase (measured by Raman) for commercial kaolins. Bars represent average standard errors for each method. The 1:1 slope line is presented for reference. See Table 1 for ID codes.

phases in a pale yellow (i.e., cream) east Georgia kaolin deposit was studied to identify causes for the variations in TiO_2 content. They found that the pale yellow coloration could be ascribed to Fe-substituted anatase in the deposit. Samples from their study were entirely cream and, therefore, they could only speculate on the nature of other Ti-phase precursors. Examination of their Figs. 2 and 3 reveals that the greatest proportion of anatase and excess TiO_2 occurs in the center of the deposits. They suggested that the changes in total TiO_2 can, in part, be attributed to the hydraulic sorting of heavy minerals associated with a transgressive sea-level depositional sequence. The relative increase in excess TiO_2 towards the center of the deposit still requires further explanation. They further suggested that oxidative fronts propagate from all sides of a kaolin deposit (i.e., from the ''outside-in''); however, a detailed mass balance study was needed to address this observation.

Published studies of actual color (i.e., redox) interfaces in kaolins are limited. Hurst and Pickering (1989) noted that Georgia kaolins are generally gray when covered by more than 15 m of overburden, and partly to entirely oxidized to cream when covered by less than 8 m of overburden. The relationships between excess TiO_2 (as seen in Fig. 7) and such factors as color, stratigraphic position, kaolinite order/disorder, and bulk chemical properties are still not clearly understood. It is expected that the development of the more precise and rapid Raman technique for detecting anatase will expedite such studies.

4. Conclusions

Quantitative analysis of anatase in Georgia kaolins by Raman spectroscopy is advantageous in that slurried solid samples pose no special problems. Accuracy and precision from the method can only be obtained if careful attention is paid to keep constant source, sample, and optical conditions. This study has identified the following relationships:

1. The Raman anatase 144 cm^{-1} band in Georgia kaolins is ubiquitous and its intensity in a single sample follows a sigmoidal function relative to weight percent solids in water-slurried preparations.
2. Anatase in Georgia kaolins has *a* lattice parameters that vary from 0.3786 to 0.3796 nm. Their crystal sizes range from 8000 to 15,000 nm and their MCL_a in the range of 80 to 160 nm. This translates to isomorphous Fe substitution in anatase ranging from 3 to 6 mol%. This narrow range of particle size, defect density, and crystal chemical variation does not appear to have any first-order effects on Raman intensity of the 144 cm^{-1} anatase band.
3. With proper considerations for source, sample, and optics, it is possible to quantify the anatase content of Georgia kaolins using Raman spectroscopy to levels of 0.3% with a standard error of $\pm 0.1\%$.
4. Total TiO_2 measures in kaolin ore cannot be used as a direct proxy for anatase content. Combined measurements of total TiO_2 and anatase provide an important constraint on Ti-phase speciation. The discrimination of Ti-phases has the potential to provide new insights to strategies for mineral separations and understanding the geological evolution of kaolin deposits.

Acknowledgements

This work was supported by a research contract between the University of Georgia Research Foundation and English China Clay International (now IMERYS Pigments and Additive Group). XRD data collection was made possible by a grant to the senior author from the National Science Foundation Instrument Facilities Program (EAR-9911501). Stephanie Meyers and Doug Hunter assisted with the Raman spectroscopy.

References

Beattie, I.R., Gilson, T.R., 1970. The single-crystal Raman spectra of nearly opaque materials. Iron (III) oxide and chromium (III) oxide. Journal of the Chemical Society. A, 980–986.

Bersani, D., Lottici, P.P., Monernero, A., 1999. Micro-Raman investigation of iron oxidized films and powders produced by sol–gel synthesis. Journal of Raman Spectroscopy 30, 355–360.

de Faria, D.L.A., Venancio Silva, S., de Oliveira, M.T., 1997. Raman microspectroscopy of some iron oxides and oxyhydroxides. Journal of Raman Spectroscopy 28, 873–878.

Farmer, V.C., 1998. Differing effects of particle size and shape in the infrared and Raman spectra of kaolinite. Clay Minerals 33, 601–604.

Grey, I.E., Reid, A.F., 1975. The structure of pseudorutile and its role in the natural alteration of ilmenite. American Mineralogist 60, 898–906.

Hinckley, D.N., 1963. Variability in "crystallinity" values among the kaolin deposits of the Coastal Plain of Georgia and South Carolina. Clays and Clay Minerals 11, 229–235.

Howard, S.A., Preston, K.D., 1989. Profile fitting of powder diffraction patterns. In: Bish, D.L., Post, J.E. (Eds.), Modern Powder Diffraction. Mineralogical Society of America, Washington, DC, pp. 217–276.

Hurst, V.J., Pickering, S., 1989. Cretaceous–Tertiary strata and kaolin deposits in the inner Coastal Plain of Georgia. Upper Cretaceous and Cenozoic Geology of the Southeastern Atlantic Coastal Plain, Field Trip Guidebook T172 28th International Geological Congress. American Geophysical Union, Washington, DC, pp. 1–22.

Hurst, V.J., Schroeder, P.A., Styron, R.W., 1997. Accurate quantification of quartz and other phases by powder X-ray diffractometry. Analytica Chimica Acta 337, 233–252.

Johnston, C.T., Sposito, G., Birge, R.R., 1985. Raman spectroscopic study of kaolinite in aqueous suspension. Clays and Clay Minerals 33, 483–489.

Kampf, N., Schwertmann, U., 1982. Quantitative determination of goethite and hematite in kaolinitic soils by X-ray diffraction. Clay Minerals 17, 359–363.

Klug, H.P., Alexander, L.E., 1974. X-ray Diffraction Procedures for Polycrystalline and Amorphous Materials. Wiley, New York. 966 pp.

Long, D.A., 1977. Raman Spectroscopy. McGraw-Hill, New York. 276 pp.

Murad, E., 1997. Identification of minor amounts of anatase in kaolins by Raman spectroscopy. American Mineralogist 82, 203–206.

Murad, E., Köster, H.M., 1999. Determination of the Ti speciation in commercial kaolins by Raman spectroscopy. Clay Minerals 34, 479–485.

Ohsaka, T., Izumi, F., Fujiki, Y., 1978. Raman spectrum of anatase, TiO_2. Journal of Raman Spectroscopy 7, 321–324.

Raman, C.V., Krishnan, K.S., 1928. A new type of secondary radiation. Nature 121, 501.

Raner, K., 1998. MacCurveFit v. 1.4—a program to fit user defined functions to a set of data points. Public domain software, 77 Therese Ave, Mt. Waverley, Vic 3149, Australia.

Schroeder, P.A., 1999. Common minerals of Graves Mountain, Georgia. Graves Mountains Georgia: Mineralogy, Economic Geology and Environmental Problems. Field Guide for the Southeastern Section Geological Society of America Meeting. Department of Geology University of Georgia, Athens, GA, pp. 12–32.

Schroeder, P.A., Ingall, E.D., 1994. A method for the determination of nitrogen in clays, with application to the burial diagenesis of shales. Journal of Sedimentary Research. Section A 64, 694–697.

Schroeder, P.A., Pruett, R., 1996. Iron ordering in kaolinites: insights from ^{29}Si and ^{27}Al NMR spectroscopy. American Mineralogist 81, 26–38.

Schroeder, P.A., Shiflet, J., 2000. Ti-bearing phases in an east Georgia kaolin deposit. Clays and Clay Minerals 48, 151–158.

Schroeder, P.A., Pruett, R.J., Hurst, V.J., 1998. Effects of secondary iron phases on kaolinite ^{27}Al MAS NMR spectra. Clays and Clay Minerals 46, 429–435.

Schwertmann, U., Cornell, R.M., 1991. Iron oxides in the laboratory: preparation and characterization. VCH Verlagsgesellschaft, Weinheim, Germany. 137 pp.

Schwertmann, U., Friedl, J., Pfab, G., Gehring, A.U., 1995. Iron substitution in soil and synthetic anatase. Clays and Clay Minerals 43, 599–606.

Singh, B., Gilkes, R.J., 1991. Concentration of iron oxides from soil clays by 5 M NaOH treatment; the complete removal of sodalite and kaolin. Clay Minerals 26, 463–472.

Skoog, D.A., Holler, F.J., Neiman, T.A., 1998. Principals of Instrumental Analysis, 5th ed. Saunders, Philadelphia, PA, pp. 15–18.

Vickers, T.J., Mann, C.K., 1991. Quantitative analysis by Raman spectroscopy. In: Grasselli, J.G., Bulkin, B.J. (Eds.), Analytical Raman Spectroscopy. Wiley, New York, pp. 107–136.

Weaver, C.E., 1976. The nature of TiO_2 in kaolinite. Clays and Clay Minerals 24, 215–218.